SECOND EUROPEAN ROTORCRAFT AND POWERED LIFT AIRCRAFT FORUM

Paper No. 26

THE INVESTIGATION OF SOME UNUSUAL HANDLING CHARACTERISTICS OF A LIGHT AUTOGYRO

J. Przybylski, R.L. Toms and I.C. Cheeseman

Department of Aeronautics and Astronautics
University of Southampton
Southampton, United Kingdom

September 20 - 22, 1976

Bückeburg, Federal Republic of Germany

Deutsche Gesellschaft für Luft- und Raumfahrt e.V.

Postfach 510645, D-5000 Köln, Germany

THE INVESTIGATION OF SOME UNUSUAL HANDLING CHARACTERISTICS OF A LIGHT AUTOGYRO

J. Przybylski, R.L. Toms and I.C. Cheeseman
University of Southampton

1. Introduction

The light autogyro, such as the Campbell-Bensen shown in Figure 1 has achieved some popularity as a private flying machine. Certain problems have been encountered and this paper details investigations carried out into some aspects of rotor behaviour. The work commenced when Mr. R.L. Toms who is the owner and pilot of Autogyro G-ARWW reported that:

1) a main rotor blade had cracked near to root. The rotor blade is of composite construction, the aerodynamic shape being formed by plywood which is bonded to a 0.32cm thick steel spar. The crack referred to above had penetrated through the wood from leading to trailing edge.

2) at particular rotor revs/min the autogyro apparently would not respond to nose down pitch inputs on the cyclic pitch.

Combining these two factors it was suggested that aeroelastic forces in the blade and control assembly may be the cause.

During these investigations the reports of three accidents to light autogyros (Refs.1,2,3) were discovered and these showed that rotor blades had deflected in flight so that they had struck the propeller and rudder. This was also true of a fourth accident at the SBAC air display at Farnborough in September 1970 - details of this accident have subsequently been given in Ref.4. Three of these accidents (Refs.1,3,4) had occurred when the autogyro had experienced reduced 'g' and when the rotor revs/min had dropped. The deflections of the rotor blade to hit the propeller and tail could not be explained on the basis of simple blade bending.

The investigation therefore started by determining the dynamic response of the rotor blades since this might explain the high root stresses and the large blade deflection necessary to cause rotor blade-propeller contact.

2. Determination of Blade Bending Frequencies

2.1 Physical characteristics of the rotor

No data was available on the aerodynamic or physical parameters of the rotor blade. The blade profile was therefore determined by means of a dial gauge mounted on vernier traverse arms situated above a surface table. Two alternative rotor blades suitable for the autogyro were examined - these were the standard Bensen wood and metal composite blade and the alternative Campbell all metal rotor blade section. The blade section was found to be constant along the span, the profile being an approximation to the NACA H.10. Details are shown in Figure 2.

The dimensions of the Bensen blade are shown in Figure 3. This shows clearly the construction of the blade at the root where it is attached to the teeter bar. This figure also shows the trim tab and the large pitching moment balance weight. This information has been used to determine the flapping stiffness and the mass distribution which are shown in Figure 4.

2.2 Determination of blade natural frequencies

2.2.1 Non-rotating condition - estimation procedures

The frequency of the various modes was calculated by several methods, first as a check on the likely differences which might occur and secondly as a comment on the accuracy of the available methods. The simplest approach is to treat the blade as if it was uniform with an equivalent stiffness and mass distribution. Bishop and Johnson[5] have produced tables which enable the solution to be determined immediately. The stiffness and mass assumption is shown in Figure 5.

The Galerkin or Rayleigh Ritz[6] energy method has been applied with the elastic and mass distribution shown in Figure 6. Yntema[6] has produced tables based on the Rayleigh energy method from which the frequency can be read. The model assumes linear mass and stiffness variations along the blade. A second version extends this model by incorporating a point mass at the tip which in this case was calculated to be equivalent to the blade balance weight. The last method used is that due to Myklestad[7] which replaces the mass distribution by a series of point masses (separated by constant stiffness sections (details are shown in Figure 6).

The results of the calculations are shown in Table 1.

2.2.2 Non-rotating conditions - experimental determination

For these tests the rotor blade was supported with its root encastre which allowed even flapping modes to be investigated. The experimental arrangement is shown in Figure 7 from which it can be seen that the blade was excited by an electromagnetic shaker connected only by piano wire. This arrangement protected the shaker from any bending and torsional forces imposed by blade couplings. The vibration spectrum from 1-40 Hz was swept slowly and the output of the accelerometer recorded. The output signal and the input were displayed on an oscilloscope to give Lissajous figures. When a resonant frequency was passed the 90° phase shift between the two signals gave a circular trace. Tests were made on two standard Bensen wood-metal composite blades and on a Campbell metal blade. The results of the test which produced the even modes are given in Table II. Comparing Tables I and II it is clear that overall the Myklestad analysis gives the best overall result. Consideration of Table II shows the flapping natural frequencies of both Bensen wood and metal and Campbell metal blades to be remarkably similar.

There is a slight difference between the two wood and metal blades which can be explained by manufacturing tolerances and similar manufacturing differences could be expected with the all metal blades.

The slight difference in frequencies between two blades which are basically interchangeable and apparently identical is considered important.

2.2.3 Rotating natural frequencies

Several of the computational methods used for the non rotating blade can be extended to apply to the rotational case. A calculation due to Langrebe[7] which aims to calculate bending moments by finding the relationship between dimensionless parameters and the corresponding empirical transfer functions determined from the analysis of mode shapes was also used. Southwell's theorem relates the non-rotating and rotating frequencies by treating the blade as a chain (i.e. zero bending stiffness) with the same mass distribution as the blade is commonly applied and was therefore included. A check was also made using a programme developed by Dr. R.F. Williams at City University[9], which is similar to Myklestad's method, but the mass is uniformly distributed along each of the finite elements.

The results of the analysis are presented in Table III. Examination shows that the Myklestad and the City University results are very similar, but that they might underestimate the increase in frequency with revs/min increase particularly in the higher modes.

A 'spoke' diagram was therefore calculated (Figure 8) which uses the static experimental values and a rev/min increase which is basically a combination of the main methods but weighted heavily by the Myklestad and City University method results.

The mode shape of the rotating blade was calculated by both the Myklestad and by City University. For the case of 300 revs/min the results are shown in Figure 9.

The position of the pusher propeller and the fin are also shown on Figure 9 and this indicates the modes which might allow the rotor to come into contact with these parts. It is however clear that if more than one mode was excited at any time then the deflection in the vicinity of the rudder could be large without extreme tip deflections.

3. An Examination of the 'Spoke' Diagram and the Implications for Blade Stresses

Figure 8 is notable because it illustrates that more than one flapping mode is excited at nearly the same rotor r.p.m. The noteworthy cases are listed in Table IV below.

The autogyro is fitted with a two bladed teetering rotor and it is therefore reasonable to expect that forces at even multiples of the rotor speed will be the more significant.

The normal take-off procedure for the autogyro without pre-spin fitted, is to spin the rotor by hand up to between 50 and 100 r.p.m. with control column fully forward and aircraft facing into wind. The control column is centralised whilst taxiing between 5-15 m.p.h. airspeed and waiting for the wind to increase rotor r.p.m. The control column is gradually eased back as the rotor gathers speed. With rotor spinning at 100 r.p.m. or more and stick fully back, taxi forward at 15-20 m.p.h. airspeed allowing rotor to gather r.p.m. When rotor reaches 200 r.p.m. open throttle fully. Rotor will continue to increase r.p.m. and nosewheel will lift off at about 300 r.p.m./20 knots. The control column is then centralised and manipulated to balance autogyro on main wheels and as airspeed builds up machine will leave the ground. Level off at

a height of 1 metre and let airspeed build up in excess of 30 knots before climbing away. The best climb out is achieved at about 35 knots.

With spin up device fitted, aircraft is faced into wind brakes on, control column fully forward, engine at fast idle. Rotor started by gentle hand swing, gear engaged, then clutch gently engaged whilst manipulating throttle. Throttle opened up slowly to increase r.p.m. Stick is now centralised, throttle opened up to give approximately 200 rotor r.p.m. when clutch and gear will trip out. Stick fully back, brakes off, throttle opened wide. As aircraft moves forward rotor will continue to increase r.p.m. and nosewheel will lift off at about 300 r.p.m./20 knots. The control column is then centralised and manipulated to balance autogyro on main wheels and as airspeed builds up machine will leave the ground. Level off at a height of 1 metre and let airspeed build up in excess of 30 knots before climbing away. Best climb out is achieved at about 35 knots.

This manoeuvre has been described in some detail because the rotor accelerates through the rotor rev/min where the modal coincidences occur (Table IV). In the case of the autogyro accidents mentioned in the introduction the rotor rev/min fell to a very low value because of a less than unit 'g' manoeuvre and hence may be subject to similar effects.

It is worthy of note that from the many test flights conducted, rates of change of rotor r.p.m. of 25 r.p.m./second were common place, 150 r.p.m./ second not unusual in a flare and rates of change of rotor r.p.m. in excess of 200 r.p.m./second experienced under certain adverse conditions.

One flight demands particular comment. The autogyro rotor was carefully tracked and inspected before the flight. Take off followed the procedure described above for aircraft without spin up device, but at rotor revs/min somewhat below 300 (pilot's reading of instrument) a violent nosewheel shimmy developed. It was possible to accelerate and take off but the violent vibration of the structure and control stick shake continued for some seconds after the autogyro was airborne. These observations were confirmed by two independant ground observers. A further six take offs were conducted with the same result. On the eighth run almost as soon as the nosewheel shimmy developed the autogyro left the ground in a steep nose up attitude and full forward movement of the control column failed to lower the autogyro's nose up attitude. The pilot noted violent control stick shake and control panel vibration, large amplitude mass balance mounting structure vibration as well as vibration of the vertical post. The autogyro was recovered by gently closing the engine throttle and allowing the aircraft to sink into the runway. It was notable that at no point did the pilot have any difficulty in keeping the aircraft in a level attitude in roll. During the flight the nosewheel tyre burst.

After the flight, inspection showed damage to the control circuit. In particular there was noticeable slack in the pitch bolt bearing under the pilot's seat and the ends of the control rod were bent (Figure 10). In addition cracking of the paint on the underside of the blade (as shown diagramatically in Figure 11) appeared during this flight - visual inspection of the blade for cracks between each flight was routine. These cracks appear where the metal spar is bonded to the plywood and hence only show on the lower surface. Combining the third even and 4th odd modes shown on Figure 9 it is seen that the cracking has occurred at points of high curvature. It is therefore extremely likely that the rotor was bending in these modes. No attempt has been made to calculate the stresses in detail since the blade loading and blade strength are not known with any confidence.

Evidence of the high vibration levels occurring at the anticipated rotor revs/min shown in Figure 8 were found by instrumenting the autogyro. Due to its extreme weight limitations and lack of suitable power supplies, the instrumentation had to be of the simplest and lightest variety. A design was made in the University of Southampton electronics laboratory which allowed four signal channels to be fed via an encoder and to be recorded as frequency modulated signals on a Phillips Cassette tape recorder. This system worked satisfactorily after normal teething troubles.

The information recorded was rotor speed (obtained by magnetic induction from two permanent button magnets on the rotor), rotor teeter angle (by means of a cam on the rotor blade yoke and a linear potentiometer), cyclic control stick position (in pitch) and strain gauge readings (via sliprings) from a rotor blade. The first three channels worked satisfactorily but the strain signals were never very satisfactory and were discounted.

The high level of vibration when the rotor revs/min shown in Figure 8 were reached was indicated by the wipers in the potentiometers which gave rotor teeter and cyclic pitch angles vibrating off their tracks to give a rapidly oscillating trace which it was impossible for the pilot or rotor to have performed.

It is therefore clear that high stresses can be generated in the rotor from these vibrations, at low revs/min and with several modes being excited at the same time. This appears from analysis of the TV film (kindly lent by CAA Accident Branch and R.A.E.) to be true in the case of the accident described in Ref.4. From the film speed it is possible to estimate the rotor revs/min and it appears that a minor strike occurs just below 300 revs/min and the major and structurally disastrous result occurs at about 180 revs/min - these results are in striking agreement with the implication of Figure 8.

4. Apparent Loss of Control Effectiveness in Pitch

It is well known that oscillation of the rotor blades at frequencies different to the rotor rotational frequency do not give rise to steady control moments. Hence the excitation of the rotor blade bending modes could not be responsible for the abnormal autogyro pitch up moment experienced. However it is significant that this motion occurred at the same time as the severe vibration mentioned above.

The flight mentioned in some detail in Section 3 provided an important clue in terms of the damage to the two control rods. A detail of the control assembly is shown in Figures 12 and 13. Examination of the mast indicated that the two control rods (only one shown for clarity in Figure 12) had deflected sufficiently to touch the mast (evidence of paint from rods on mast). It appeared therefore that the two push rods had executed violent oscillations which would have effectively shortened their mean length and hence the rotor head would be tilted back compared to its position when the rods were not vibrating and the pilots control stick fixed.

The natural frequency of the control rods treated as light alloy tubes freely pinned at the ends was estimated and found to be 25.2Hz for the first and 100Hz for the second mode. It will be noted from Figure 8 that the third even mode occurs at 156 rads/sec (24.83Hz). This suggests that the first mode could be excited by inputs from the third even blade flapping mode which is driven by 6/rev aerodynamic inputs. The near agreement of the control rod

natural frequency and the blade flapping mode must be qualified because the control rod can be under compression or tension depending on the conditions in the rotor, the autogyro C of G position etc. Not shown in Figure 12 is the bias spring which is attached from the yoke at the top of the control rod to the mast and tends to pull the rotor head backwards. Clearly therefore the exact natural frequency of the control rod will depend on the stick position, the rotor lift force and the bias spring stiffness. It is clear from experience with G-ARWW that the coincidence of these conditions can occur even when the pilot is apparently making exactly the same manoeuvre due to, for example, changes in the centre of gravity, flight manoeuvre or changes to the central bias spring. It is noted that in the accident reported in Ref.2, the bias springs were extended to twice the normal length due to the fitting of new metal rotor blades.

The differences noted in the natural frequencies between blades (Table II) which are basically interchangeable can be extremely important as the control rod tube resonance appears to be sharp. Hence nominally identical aircraft may or may not exhibit these effects as well as individual aircraft showing these effects only on some flights.

It will be noted that due to the locking of the rotor and control rod vibration, both control rods will vibrate in phase. Hence the rotor tilt will only occur in pitch and not in the roll plane, this is in agreement with the pilot's observations in the incident recorded in Section 3.

It is apparent that the rotor is likely to strike the propeller or rudder when the pilot has full aft cyclic control applied when the control rod shortening will produce maximum rearward tilt of the rotor head. Such a case will arise when the pilot is trying to recover from a manoeuvre like a bunt as was apparently the case in the accidents recorded in References 1, 3 and 4.

5. Conclusions

The design of the rotor blades for the gyrocopter give rise to coincidences of flapping natural frequencies excited by low order aerodynamic excitation. Combination of these modes can lead to large excursions of the blade from its undeflected shape in the vicinity of the propeller and rudder and could explain the cases of blade strike reported in three fatal accidents. The coincidence at rotor speed just below that recommended in one take-off technique is most important.

The first order bending frequency of the control rods may be the same as the third even blade bending mode excited by the 6/rev aerodynamic input. In this case the rotor head tilts rearward giving a nose up pitch to the autogyro.

6. Recommendations

The redesign of the control assembly to remove any possibility of the control rod natural frequency being excited by the rotor forces is strongly recommended.

7. Acknowledgment

The authors record with pleasure the financial assistance received from the Handly Page Memorial Fund of the Royal Aeronautical Society.

References

1. Brooklands Mosquito MkII Gyroplane G-AVYW. Report on the accident at Tine Side Airport, Middleton St. George, Co. Durham, 9th March 1969. Civil Aircraft Accident Report 16/71, H.M.S.O.

2. Bensen B8M Gyrocopter G-AWBO. Report on the accident half a mile east of Mount Karnon, Isle of Man on 15th September 1969. Civil Aircraft Accident Report 6/72, H.M.S.O.

3. Brookland Hornet Gyrocopter G-AWTZ. Report on the Accident at Woodford Aerodrome, Cheshire on 27th June 1970. Civil Aircraft Accident Report 5/72, H.M.S.O.

4. Wallis WA 117 Autogyro G-AXAR. Report on the accident at Farnborough, Hants on 11th September 1970. Civil Aircraft Accident Report 7/74, H.M.S.O.

5. R.E.D. Bishop and D.C. Johnson, The Mechanics of Vibration (Chapter 7). Cambridge University Press 1960.

6. R.T. Yntema, Simplified Procedures and Charts for the Rapid Estimation of Bending Frequencies of Rotating Beams. NACA TN 3459, 1955.

7. N.O. Myklestad, Vibration Analysis. McGraw-Hill, 1944.

8. A.J. Langrebe, Simplified Procedure for Estimating Flapwise Bending Moments on Helicopter Blades. NASA CR 1440, Oct. 1969.

9. R.F. Williams, Method unpublished, but referred to in Helicopter Dynamics by A.R.S. Bramwell, published by Arnold (page 313).

Table I

Flapping Natural Frequency (radians/sec)

Mode	Calculated Method				
	Bishop & Johnson	Galerkin	Yntema (1)	Yntema (2)	Myklestad
1st even	6	8	6.9	3	6.2
2nd even	36	-	39	27.3	41.2
3rd even	101	-	106	84.3	101.2
4th even	197	-	-	-	189.2
1st odd	-	-	-	-	0
2nd odd	-	17.8	26.6	18	24.5
3rd odd	-	-	86.5	67	73.3
4th odd	-	-	186	148	136.3

NB Yntema (1) - uniform line density and flapping stiffness

Yntema (2) - Yntema (1) plus tip mass.

Table II

Experimentally Determined Flapping Natural Frequency (radians/sec)

Mode	Blade		
	Wood and metal blade I	Wood and metal blade II	Campbell metal blade
1st even	6.85	6.63	8 8
2nd even	44	43.9	44.3
3rd even	114.2	112	119..
4th even	200.5	194.8	226
5th even	312	307	---

Table III

Calculated Rotating Blade Natural Frequencies (rads/sec)

Mode	Method: / Revs/min:	Galerkin 200	Galerkin 400	Yntema[1] 200	Yntema[1] 400	Yntema[2] 200	Yntema[2] 400	Myklestad 200	Myklestad 400	Southwell 200	Southwell 400	Langrebe 200	Langrebe 400	City 400
1st even		26.4	50.9	24.3	47.1	23.2	40.3	24.1	46.1	22	42	22.8	43.5	44.7
2nd even		--	--	63	107	78	130.7	74.4	127.5	51	68	63.6	110	125.9
3rd even		--	--	133	192	157	247	134.7	182.5	124	153	136	200	207.4
4th even		--	--	--	--	--	--	225.0	270.0	208	243	226	315	316.8
1st odd		--	--	--	--	--	--	21.15	42.1	--	--	--	--	41.9
2nd odd		46.5	87.8	56.1	103.5	73	124	62.8	128.2	--	--	58.6	106	115.3
3rd odd		--	--	119	186	147	239	113.2	160.7	--	--	121	192	191.0
4th odd		--	--	219	296	243	370	176.7	247.4	--	--	213	304	279.3

Table IV

Coincidences of Bending Modes at Approximately the Same Rotor revs/min

Rotor rev/min				
141-155	(Mode	2nd even	3rd odd	3rd even
	(Excitation force/rev	4	7	8
175-189	(Mode	2nd odd	3rd odd	3rd even
	(Excitation force/rev	3	6	7
247-248	(Mode	3rd even	4th odd	
	(Excitation force/rev	6	8	

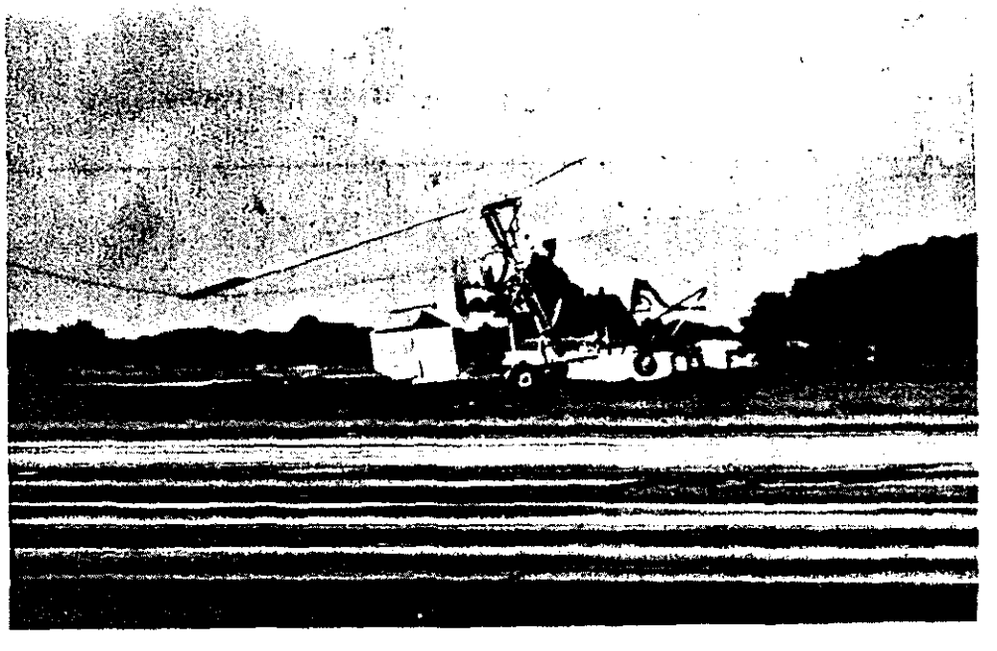

Fig.1 CAMPBELL-BENSEN AUTOGYRO

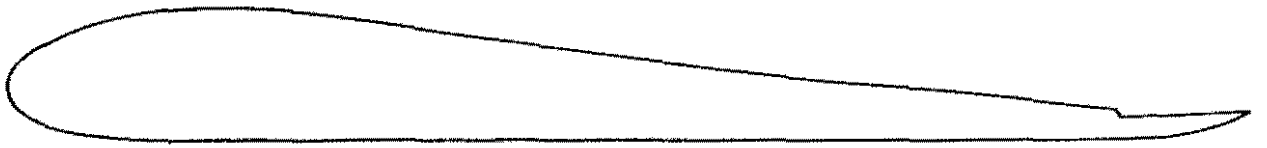

Bensen wood and metal composite rotor blade section.

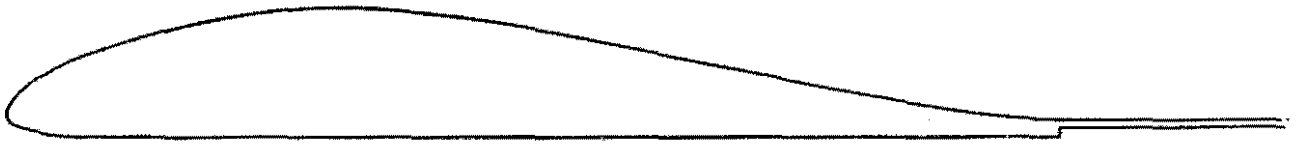

Campbell all metal rotor blade section.

FIG. 2 MODIFIED H10 AEROFOIL SECTIONS

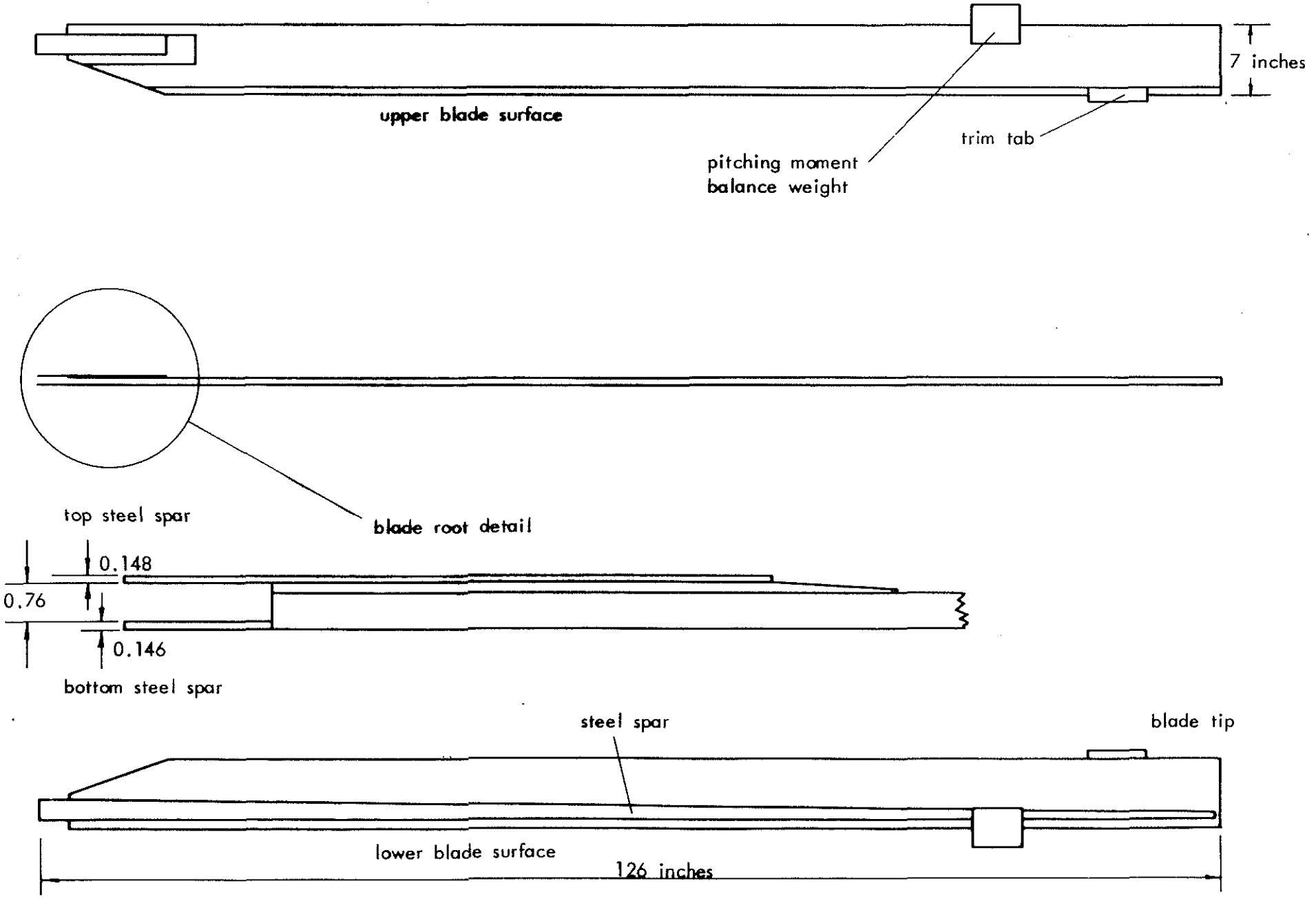
7 inches
upper blade surface
trim tab
pitching moment
balance weight
top steel spar
blade root detail
0.148
0.76
0.146
bottom steel spar
steel spar
blade tip
lower blade surface
126 inches

FIG 3.

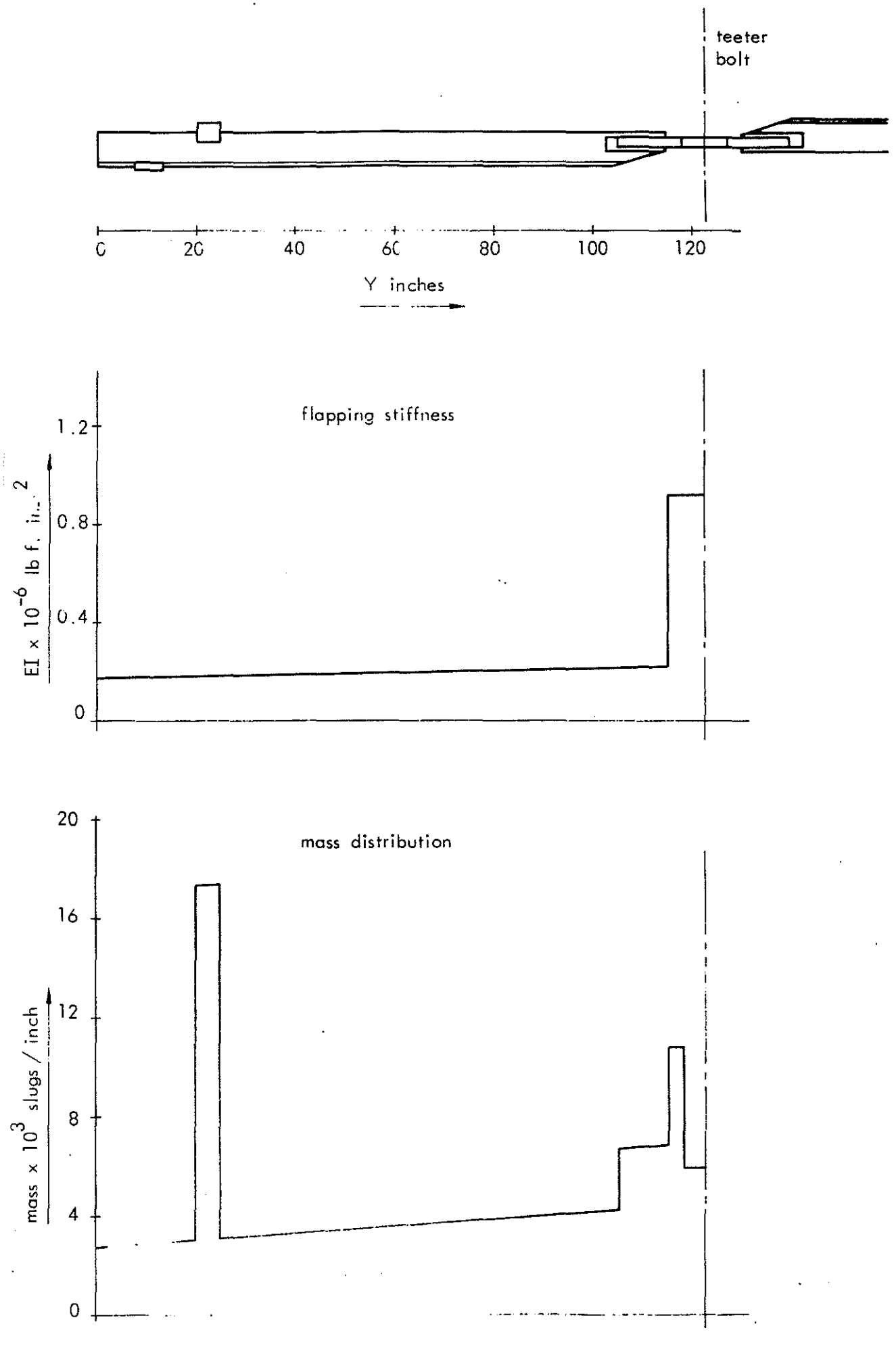

FIG. 4 ESTIMATED STRUCTURAL PROPERTIES OF THE ROTOR BLADE

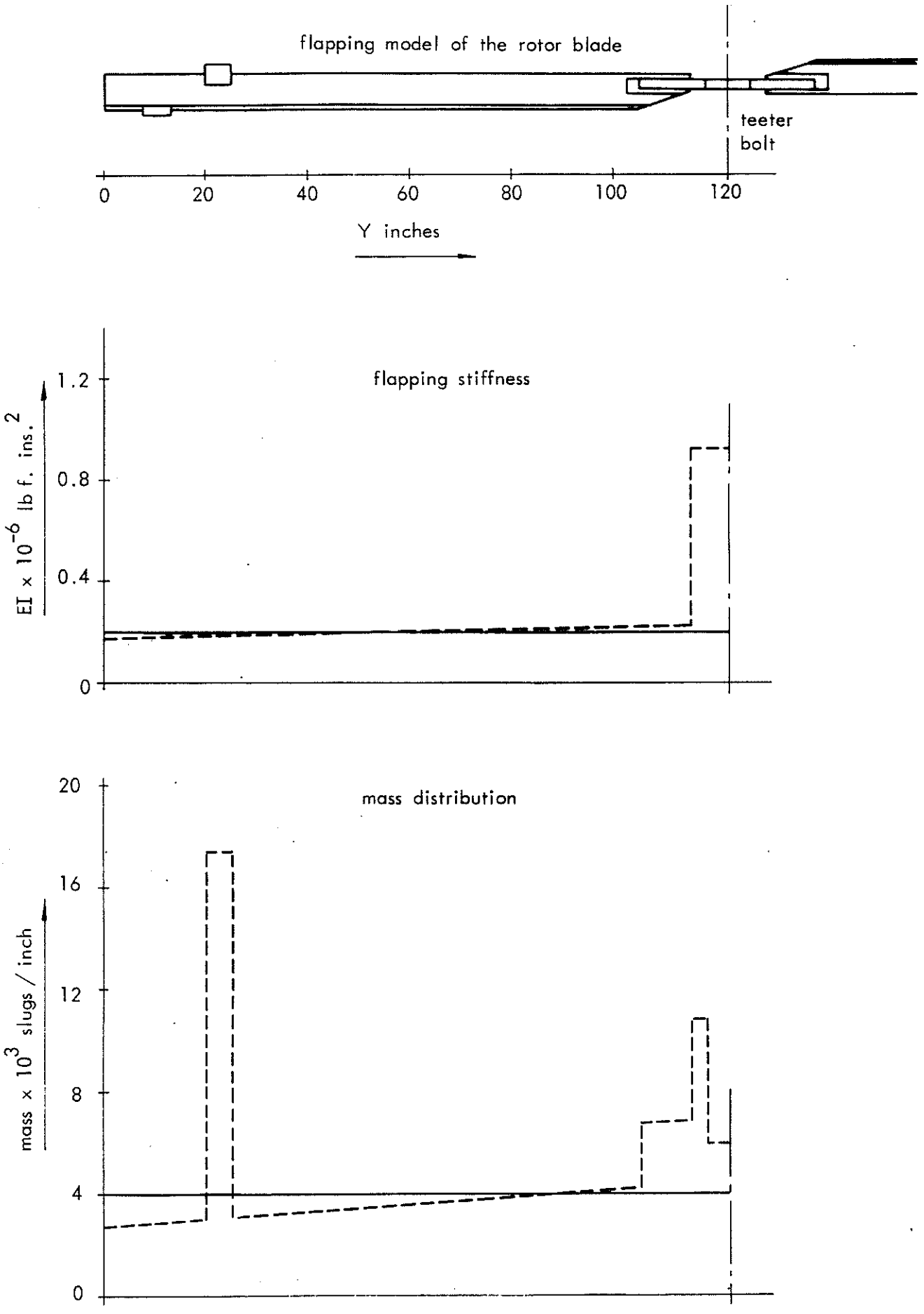

FIG. 5. BISHOP AND JOHNSQN AND LANGREBE METHOD

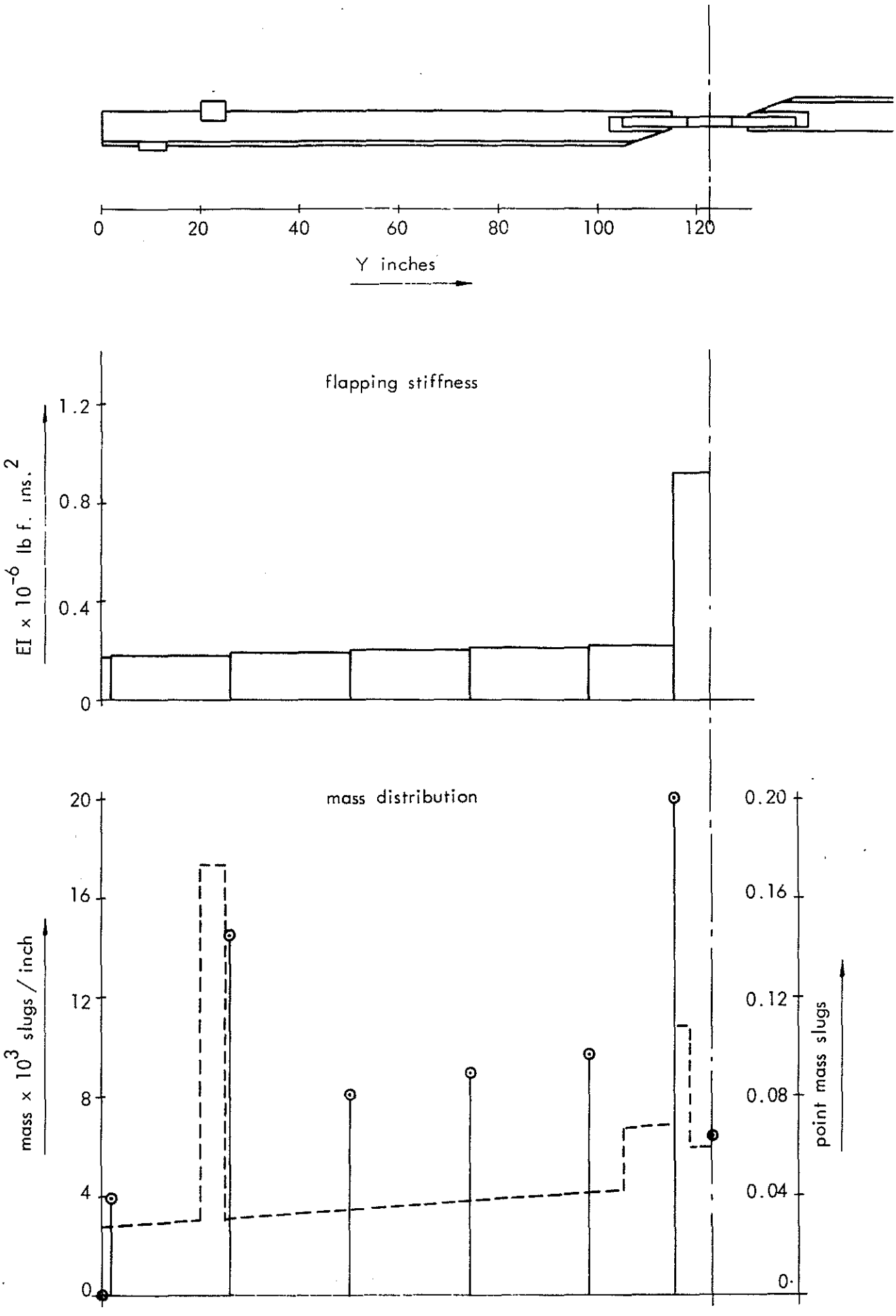

FIG. 6 MYKLESTAD FLAPPING MODEL OF THE ROTOR BLADE

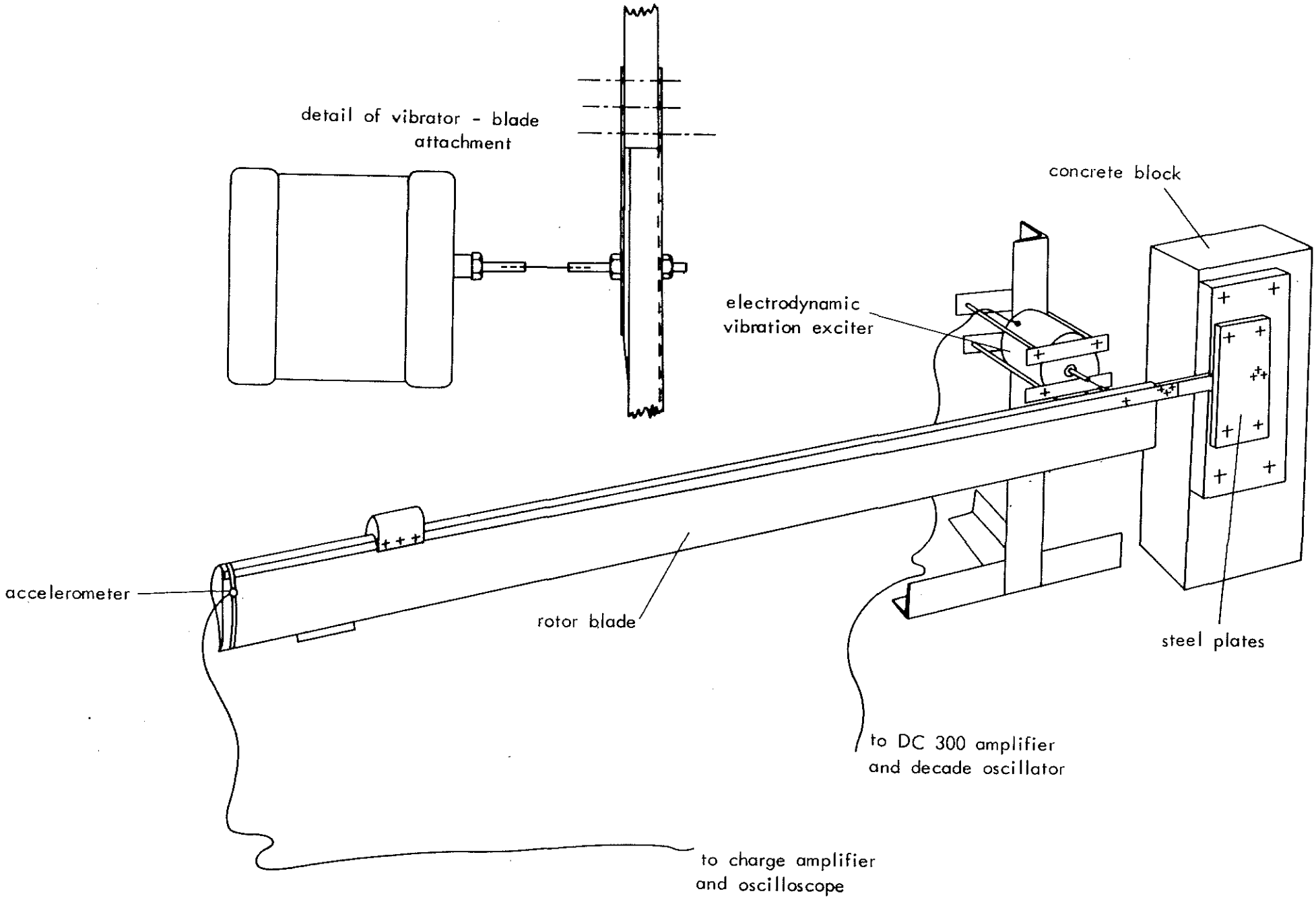

FIG. 7 EXPERIMENTAL SET UP FOR THE VIBRATION TESTS ON THE ROTOR BLADES

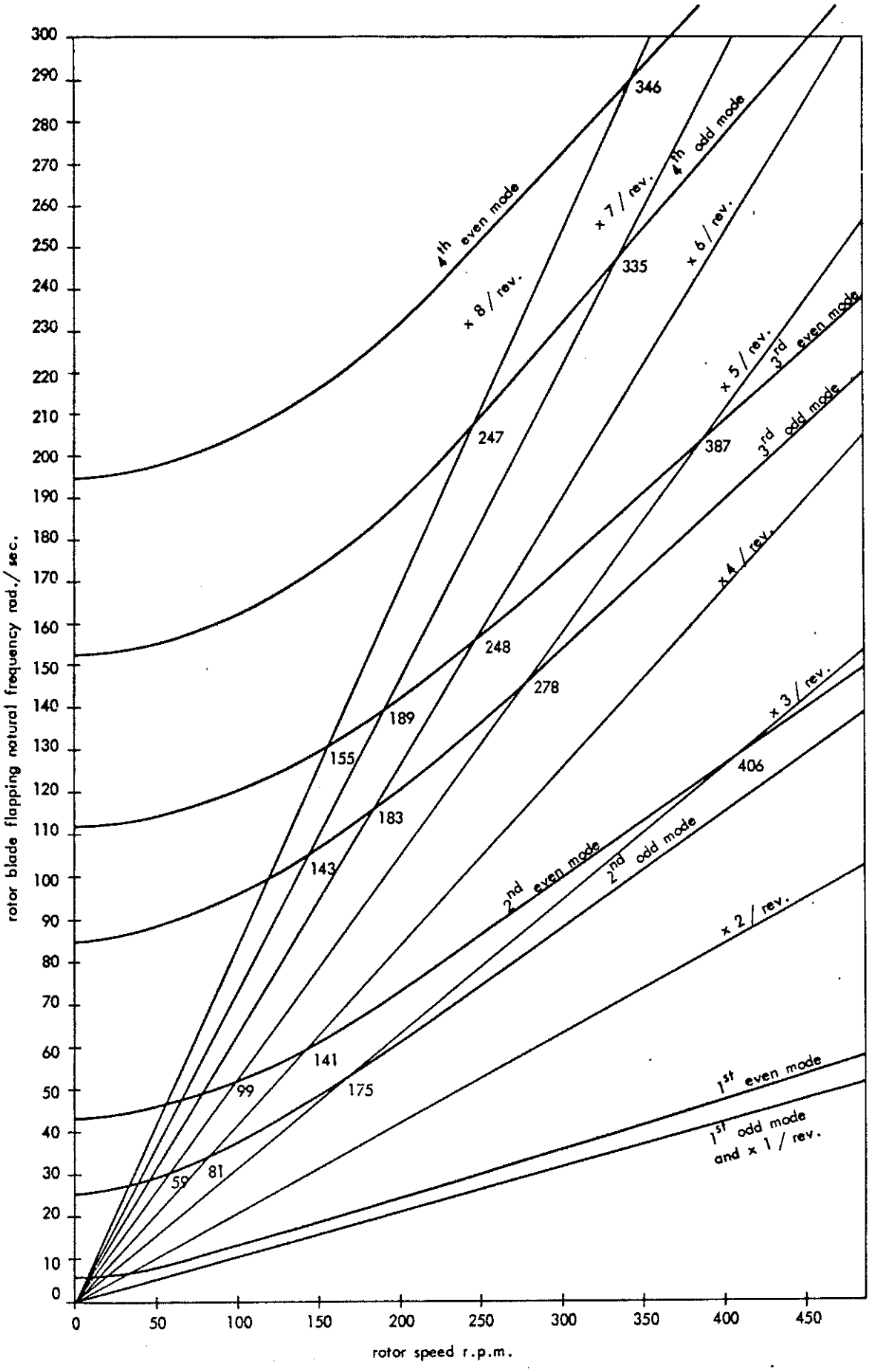

FIG. 8 SPOKE DIAGRAM

STATIC EXPERIMENTAL RESULTS AND ESTIMATED DYNAMIC RESPONSE

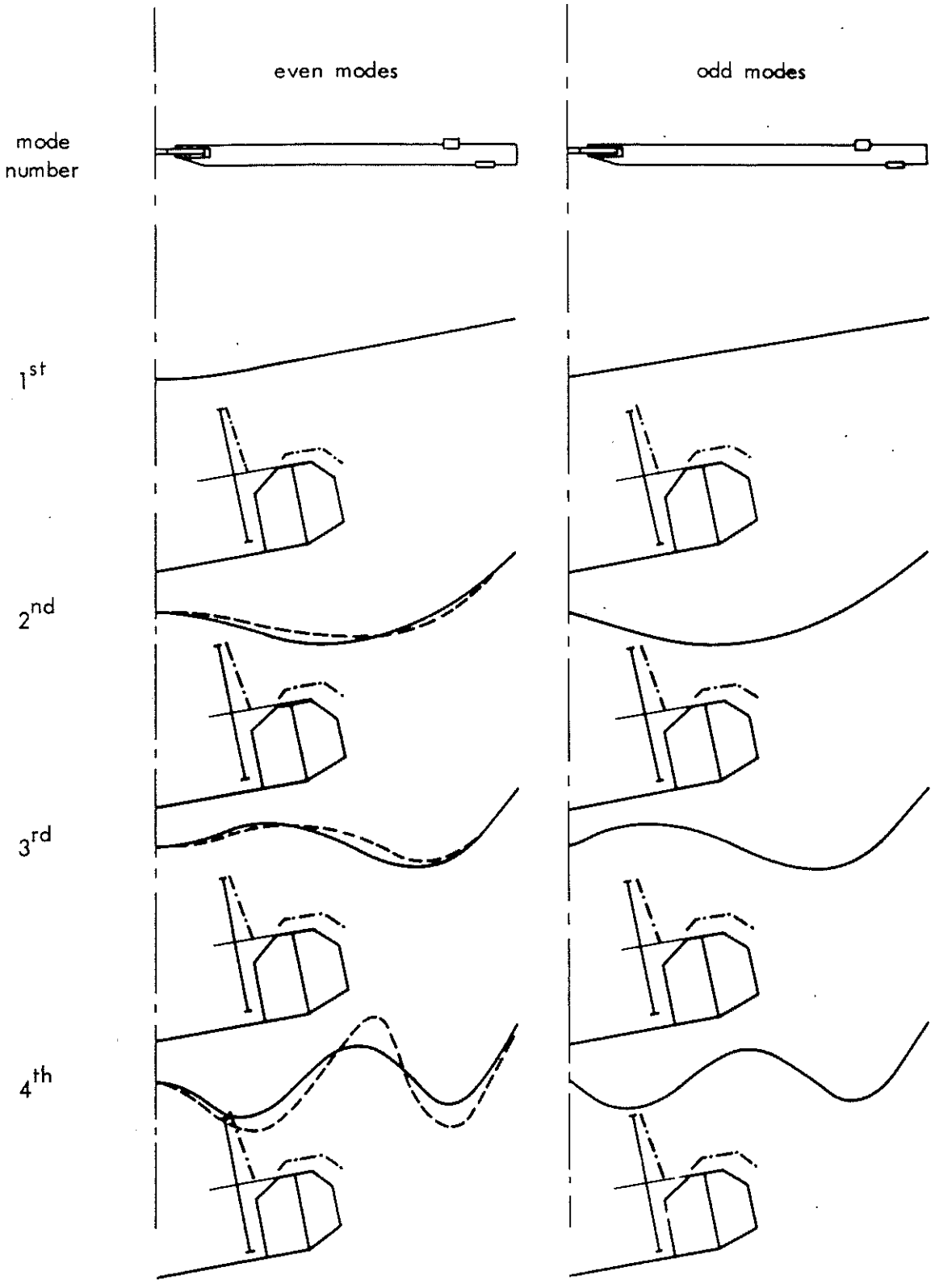

FIG. 9 FLAPPING VIBRATION MODES FOR THE BENSEN COMPOSITE WOOD AND METAL ROTOR BLADE

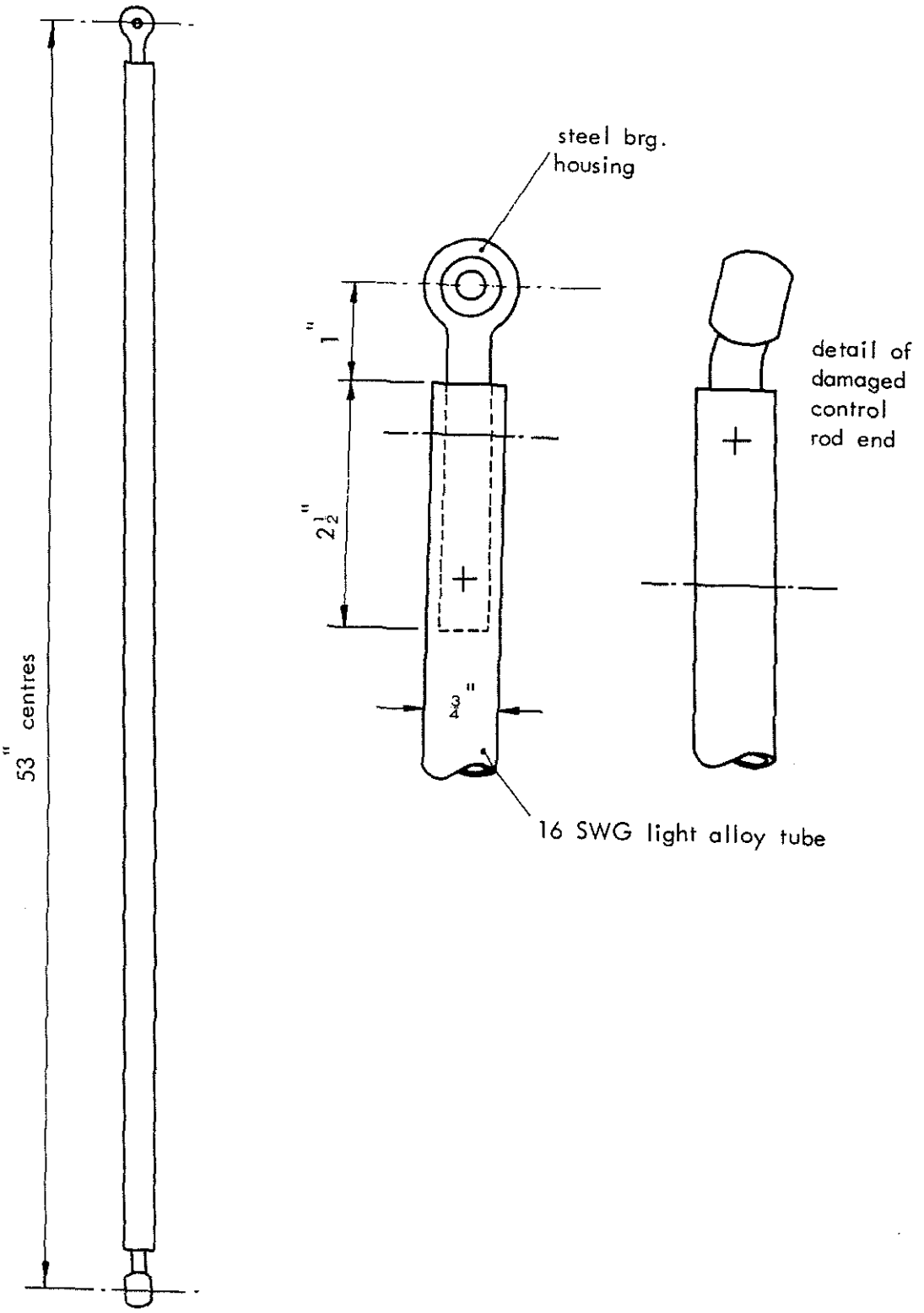

FIG. 10 CONTROL RODS AFTER FLIGHT ON 18-7-74

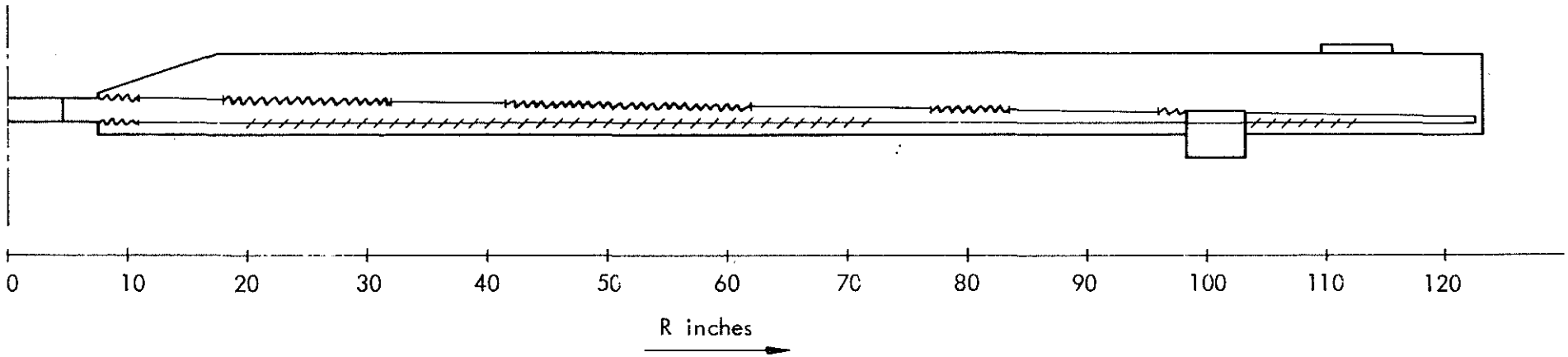

FIG. 11 POSITION OF PAINT CRACKS ON THE ROTOR BLADE AFTER THE FLIGHT ON 18-7-74

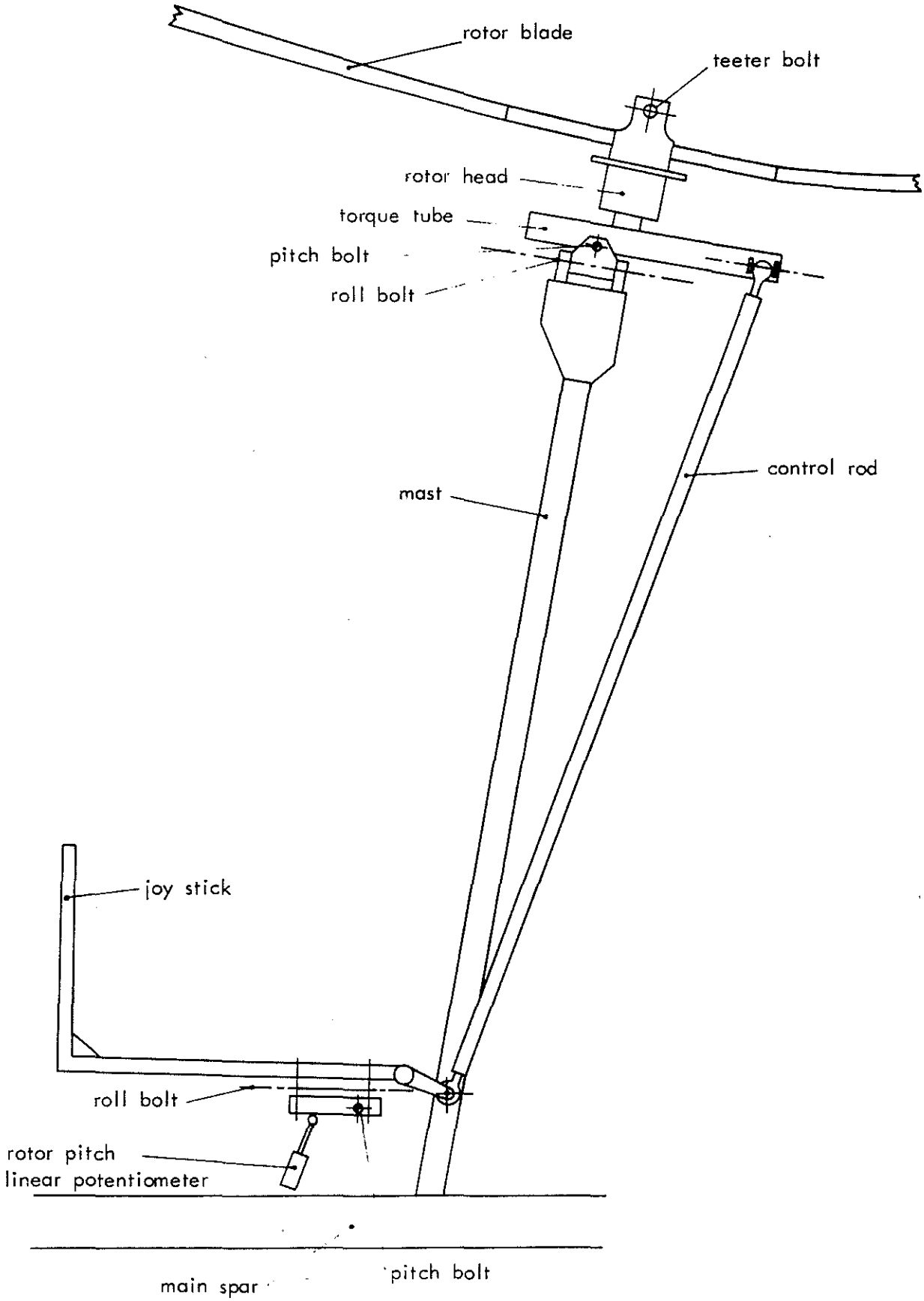

FIG. 12 SKETCH OF CONTROL LINKAGE AND ROTOR PITCH INSTRUMENTATION

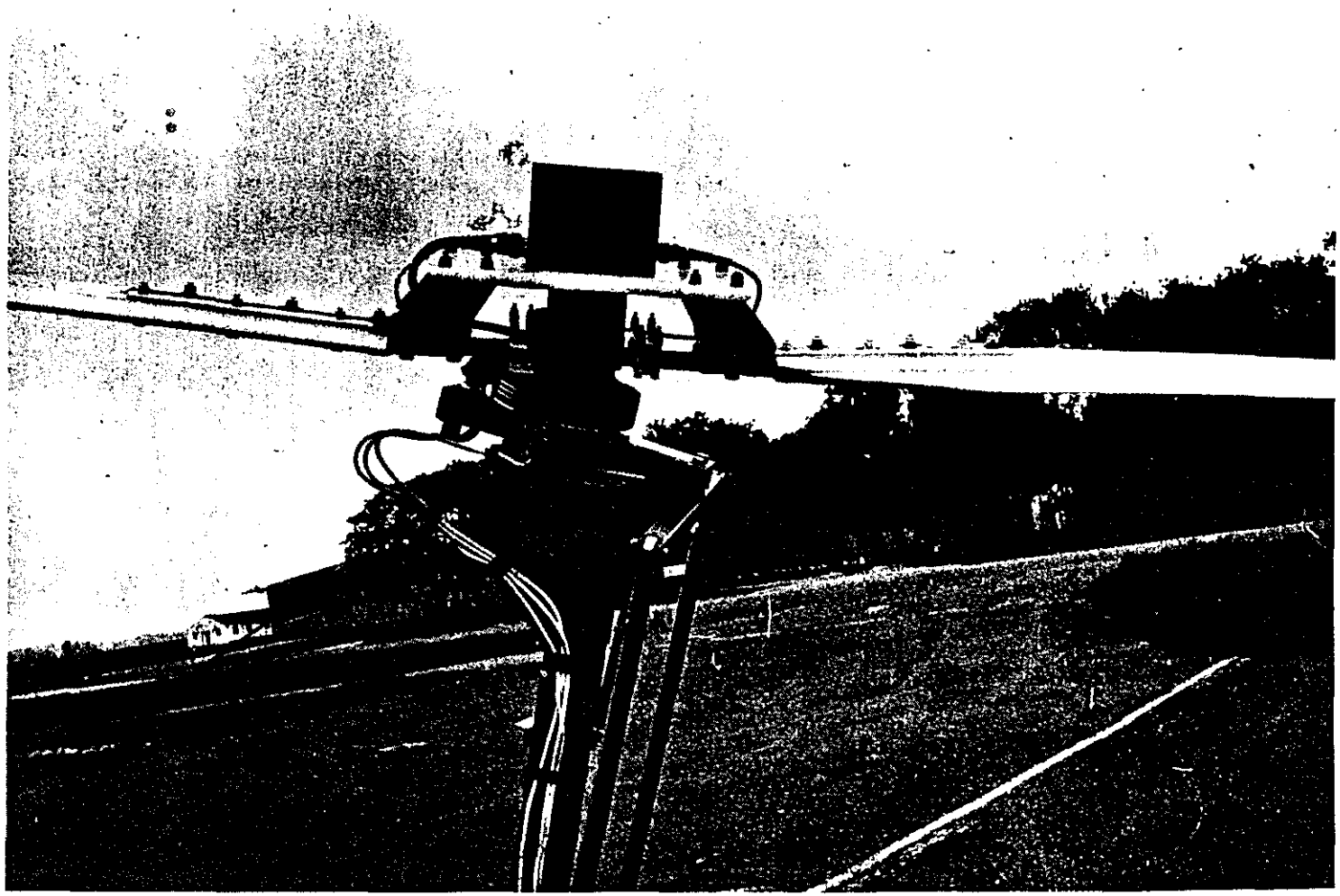

Fig.13 ROTOR HEAD AND CONTROLS OF AUTOGYRO